Enhancing Simulation Environments for The Artificial Pancreas

Ali Emami

Master of Science

School of Computer Science

McGill University
Montreal, Quebec
2016-01-06

A thesis submitted to McGill University in partial fulfillment of the requirements of the degree of Master of Science

TABLE OF CONTENTS

ACKNOWLEDGEMENTS

First and foremost, I thank my supervisors, Joelle Pineau and Ahmad Haidar for their guidance, support, and most importantly, trust during the last few years. I have profoundly enjoyed working in both the Reasoning and Learning Lab as well as The Institut De Recherches Cliniques De Montreal (IRCM), the latter of which under the guidance of Remi Rabasa-Lhoret.

Additionally, the help from Dr. Rabasa-Lhoret's team at the IRCM has been essential to the realization of my thesis. In particular, I want to thank the team of nurses and clinicans at the IRCM, including but not limited to Virginie Messier, Nadine Taleb, Corrine Suppere, Maryse Dallaire, and Annie Magnan, for their hard work, support, and friendship.

I am also grateful for the financial support I received from both the Natural Sciences and Engineering Research Council of Canada and the Fonds de Recherche Sante Quebec.

ABSTRACT

The dual-hormone artificial pancreas is an emerging technology to treat type 1 diabetes. It consists of a glucose sensor, infusion pumps, and a dosing algorithm that directs hormonal delivery. Pre-clinical optimization of dosing algorithms using computer simulations has the potential to accelerate the pace of development for this technology. Current simulation environments are far from complete, and in the following thesis we extend them to include two components: a glucose sensor model that accounts for dropouts of sensor readings, and a glucagon action sub-model. To develop the glucose sensor model, potential drop-outs were augmented to an existing model and their incidences and parameters were estimated simultaneously with the parameters of the model using the Bayesian approach. Drop-outs and model parameters were estimated from data collected from 15 subjects with type 1 diabetes who underwent an artificial pancreas study. Model fitting and parameter estimates were contrasted between the enhanced model and the one-compartment existing model. The enhanced model improves fitting of glucose levels and should allow more realistic simulations. In developing the glucagon action sub-model, we considered eight candidate models of glucagon action featuring a number of possible characteristics: insulin-independent glucagon action, insulin/glucagon ratio effect on hepatic glucose production, insulin-dependent suppression of glucagon action, and the effect of rate of change of glucagon. To assess the models, we used measurements of plasma insulin, plasma glucagon, and endogenous glucose production collected from experiments involving 8

subjects with type 1 diabetes who received four subcutaneous glucagon boluses. We estimated each model's parameters using a Bayesian approach, and the models were contrasted based on the deviance information criterion. The model achieving the best fit features insulin-dependent suppression of glucagon action and incorporates effects of both glucagon levels and its rate of change.

ABRÉGÉ

Le pancréas artificiel à double hormone est une technologie émergente pour soigner le diabète de type 1. Il se compose d'un capteur de glucose, pompes de perfusion, et un algorithme de dose qui contrôle la distribution des hormones. L'optimisation préclinique des algorithmes de dosage en utilisant les simulations par ordinateur a le potentiel d'accélérer le rythme de développement de cette technologie. Les environnements de simulation en cours sont loins d'être complets, et dans la thèse suivante on propose d'inclure deux constituants: un modèle de capteur de glucose qui explique les données manquantes des interprétations de capteurs, et un sous-model de l'action du glucagon. Afin de développer le modèle de capteur de glucose, les donnés manquantes ont été ajoutées à un modèle existant et leur incidence et paramètres sont estimés simultanément avec les paramètres du modèle en utilisant l'approche Bayesian. Les paramètres du modèle ont été estimés en utilisant des données de 15 sujets avec le diabète de type 1. L'adéquation du modèle d'estimation des paramètres est contrasté entre le modèle amélioré et le modèle existant à compartiment unique. Le modèle amélioré optimise l'estimation des niveaux de glucose et devrait permettre des simulations plus réalistes permettant d'évaluer les systèmes de pancréas artificiels. En développant le sous-modèle de l'action de glucagon, on utilise des donnés provenant de sujets présentant plusieurs des caractéristiques possibles : action de glucagon non insulinodépendant, l'effet de l'insuline/glucagon sur la production de glucose hépatique, la répression non insulinodépendante de

l’action de glucagon, et l’effet du taux de changement de glucagon. Dans le but d’évaluer les modèles, on considère les mesures de l’insuline plasmatique, glucagon plasmique, et la production de glucose endogène collectées à partir de huit sujets avec le diabète de type 1 qui ont reçus quatre bols alimentaires de glucagon sous-cutanés. On estime les paramètres de chaque modèle utilisant une approche Bayesian, et les modèles sont comparés en utilisant le critère de déviance. Le modèle qui correspond le mieux avec les données disponibles est celui incluant la répression de l’action de glucagon et incorporant l’effet du glucagon ainsi que son taux de changement.

LIST OF TABLES

LIST OF FIGURES

CHAPTER 1
Introduction

1.1 Type 1 Diabetes

Insulin is a hormone secreted by pancreatic beta cells that promotes glucose utilization with which glucose concentration in the blood is reduced [1]. Glucagon, on the contrary, is a hormone secreted by pancreatic alpha cells which promotes the conversion of hepatic glycogen into glucose, increasing glucose concentration in the blood. In a healthy individual, the blood glucose concentration is closely managed by both of these hormones.

Type 1 diabetes (T1D) is a chronic disease that leads to the autoimmune destruction of pancreatic beta cells, resulting in the absence of insulin secretion in the pancreas [2]. Accounting for 5-15% of approximately 366 million worldwide patients with diabetes, the incidence of T1D is increasing at a rate of 3.9% per year [3].

The discovery of Insulin in the early 1920's allowed for the treatment of T1D, transforming it from a fatal condition into a disease requiring lifelong treatment. This treatment, known as insulin replacement therapy, requires either multiple daily injections of insulin or continuous subcutaneous insulin infusion via a pump, called insulin pump therapy. Glycemic levels should be tightly controlled, given that repeated occurrence of high glucose levels (hyperglycaemia) leads to long-term complications such as heart disease, kidney failure, nerve damage, and blindness [4].

Insulin pump therapy features insulin delivered in a continuous manner through a portable pump [5], and requires frequent finger-stick blood glucose measurements, calculating the carbohydrate content of each meal, and adjustment of various factors including insulin sensitivity (how much glucose is dropped after the delivery of 1 unit of insulin). This treatment option improves glycemic control compared to multiple daily injections in most T1D patients [6].

The mid 2000's introduced real-time continuous glucose monitoring systems, also known as continuous glucose sensors. While being less accurate than conventional glucose meters, these sensors measure, on a continuous basis, the blood glucose despite being minimally invasive. Consisting of a fine disposable probe and transmitter implanted under the skin, the system links wirelessly to a handheld device that analyses the received data and displays the glucose levels to the patient. These systems are being improved rapidly and are progressively showing greater accuracy.

Despite the advances above, insulin pumps and continuous glucose sensors are far from perfect, as glucose control remains problematic and most patients do not achieve glucose targets [7], [8]. In addition, hypoglycemia (low blood glucose) secondary to insulin therapy may occur and lead to seizures, unconsciousness, or even death [9].

1.2 Closed-Loop Systems in Type 1 Diabetes

Despite the remarkable progress observed in sensors and pump technologies, the desire to combine the interface between the two in an automated manner has recently led to the development of closed-loop delivery systems (often called the "Artificial Pancreas"). In this system, subcutaneous glucose sensor readings are continuously transmitted to a mathematical dosing algorithm which dynamically controls the rates of hormonal infusion pumps (Fig 1.2) Two configurations of the artificial pancreas, the single-hormone (insulin-only) and the dual-hormone (insulin and glucagon), have been shown to offer tighter glucose control compared to conventional pump therapy [8]. However, the addition of glucagon has the potential to further lower hypoglycaemia at the expense of increased costs and device complexity.

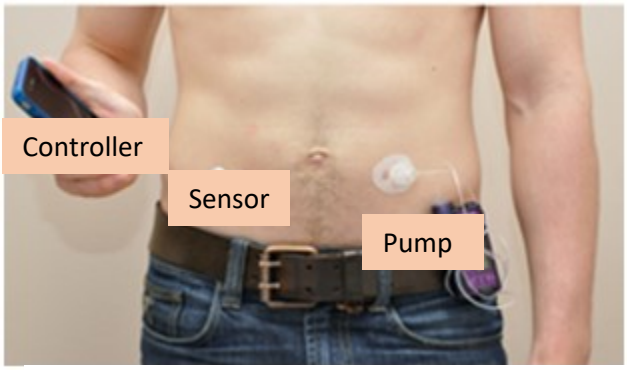

Figure 1.1: Closed-Loop Delivery System

Despite the momentum that the Artificial Pancreas has gained and its projection as the most promising treatment option for patients with type 1 diabetes, a few major milestones stand in its way. First, to evaluate the safety and efficacy of such systems, in-patient clinical trials are necessary. These will allow

for the testing of the system in controlled conditions as well as for improving the dosing algorithms. Given that clinical trials are time-consuming and expensive, computer simulation environments can be developed to further test the system before moving onto less controlled clinical environments. This would, naturally, allow testing the system under extreme conditions (hardware failure, sensor malfunction, stress, etc) that would not otherwise be allowed in clinical studies due to ethical reasons. It is important to note that clinical and simulations studies improve each other in an iterative manner; data collected from clinical studies are used to improve the realism of the simulation environment, which can be used to improve the dosing algorithm that can, in turn, be used to collect more clinical data. In order for the simulation environment to be given regulatory approval (Health Canada, Federal Drug Administration), validation needs to take place. This is performed by comparing the environment's predictions against a clinical study evaluating overnight closed-loop insulin delivery.

Before moving to out-patient studies, closed loop devices also need to be given regulatory approval Finally, following these out-patient studies, long term home studies will be needed to conclusively contrast the closed loop system against conventional treatments.

1.3 Simulation Environments

Clinical trials are an integral part of the development process of closed-loop systems but are time-consuming, resource demanding, and costly [10], [11]. Pre-clinical testing in a computer-simulation environment accelerates development and facilitates optimization of dosing algorithms. Simulation environments are

composed of a mathematical model of glucose regulation representing "virtual patients", a glucose measurement model, and the insulin delivery model, all described by a set of differential equations along with parameters that differ from one patient to another [12]. The structure of the differential equations defines the relationship between physiological variables, such as insulin, glucagon, blood glucose, sensor glucose, insulin sensitivity, total daily dose (of insulin), meal sizes, exercise, and other demographic variables (age, weight, duration of diabetes). Many of the key physiological variables exhibit both inter- and intra-patient variability (with the former being more prominent). For example, day-to-day variations of insulin sensitivity in Type 1 individuals in one study showed a coefficient of variation of 13%, with inter-patient coefficient of variation of around 25% [13]. Total daily dose of insulin, another important variable, is known to show ten-fold intra- patient variability (0.2 units/kg/day to 2 units/kg/day). Furthermore, factors including age, weight, time of day, and activity level may largely affect parameters including insulin and glucagon sensitivity. The primary goal of simulation environments is to mimic reality as closely as possible; very much as is the goal of a flight simulator. For example, the structure of the environment should define that insulin reduces glucose levels, but that its action is modulated by insulin sensitivity (e.g. the ability of insulin to produce its biological effect). Likewise, it should mimic the characteristics of a sensor reading (i.e its incapacity to entirely correspond with blood glucose levels, either through sensor underreading, overreading, physiological delays, or other eccentricities). All together, these components combine to produce an

environment that can very much simulate that of a clinical study. The simulator would be provided (or can generate) multiple virtual patients, described by their own characteristic parameters, and for a specification of experimental protocol, glucose measurement and insulin delivery model, as well as dosing algorithm used, would output a comprehensive analysis of study results. As with the clinical setting, the algorithm's performance through the simulation environment is evaluated on the basis of time spent in a safe glycaemic range (4-8 mmol/L) and glucose variability.

1.4 Thesis Contribution

In the following thesis, we present models that contribute to the completion of the simulation environments that test the Artificial Pancreas. In particular, we present a detailed overview of the methodology and results of two such models we have developed: a glucose sensor model that accounts for drop-outs in sensor models, and an enhanced glucose regulation model. The rest of this thesis is organized as follows. Chapter 2 provides a literature review of work done towards developing current simulation environments, as well asrelated work regarding models describing certain components of these environments. It also introduces the technical background for our modelling tasks and describes the statistical inference methods and software used to solve it. Chapters 3 and 4 highlight the experiment and results of the two studies performed, the former of which can be found published in [14], and the latter found published in [15]. Finally, Chapter 5 concludes and discusses the work presented in this thesis before outlining avenues for future work.

1.5 Authors Contributions to the Manuscripts

"Enhancing Glucose Sensor Models: Modeling the Drop-Outs," A. Emami, R. Rabasa-Lhoret, and A. Haidar:

My contributions to the manuscript included the development and evaluation of the method, interpretation of the results, and the writing of the manuscript. Remi Rabasa-Lhoret and Ahmad Haidar supervised the work.

"Modelling Glucagon Action in Patients with Type 1 Diabetes," A. Emami, J. El Youssef, R. Rabasa-Lhoret, J. Pineau, J. Castle, and A. Haidar:

My contributions to the manuscript also included the development and the evaluation of the method, interpretation of the results, and the writing of the manuscript. I was not involved in the design or conducting of the clinical study, which was performed by co-authors J. El Youssef, and J. Castle. J. Pineau and Ahmad Haidar supervised this work.

CHAPTER 2
Problem Domain

In the following chapter, we review the most recent efforts to complete the simulation environments that test the Artificial Pancreas, followed by some technical background for the thesis. Particularly, in the first section, we review three major simulation environments proposed by various teams that contain three fundamental components: the glucose regulation model, the glucose measurement model, and the insulin delivery model. In the two subsequent sections, we review work being done on developing and enhancing specifically two of these components: the sensor model, and the glucose regulation model. For each of these components, we describe some limitations that have yet to be addressed and outline how we seek to resolve them in our thesis. In the final sections, we describe some of the statistical inference methods by which we develop and enhance these models, as well as the software used to implement them.

2.1 Current Simulation Environments

Three major simulation environments have thus-far been developed to test the Artificial Pancreas [11], [16], [17]. Kovatchev et al. [17] created an environment of 300 virtual type 1 diabetes patients. Using glucose fluxes obtained in healthy individuals, parameters were estimated for a complex model of glucose regulation they proposed, and then altered to represent type 1 diabetes subjects. Briefly, their model assumes that the insulin and glucose subsystems are connected to each other via the control of insulin on endogenous production.

The main processes that govern the model are endogenous glucose production, glucose rate of appearance, and glucose utilization. The suppression of endogenous glucose production is assumed to have a linear affect on plasma glucose and portal insulin concentration.

Another such simulation environment was developed by Medtronic [16], based on Bergman's minimal model [18], an early model describing insulin's effect to increase glucose uptake and decrease endogenous glucose production via insulin sensitivity. In this environment, compartmental models were used to describe the pharmacokinetics of subcutaneous insulin and glucose concentration following a meal. Model parameters were obtained by fitting glucose data in 10 type 1 diabetes subjects who underwent closed-loop experiments. Data was fitted using nonlinear least squares regression.

More recently, a simulation environment of 18 virtual subjects has been proposed by Wilinska et al [11], combining a mathematical model of glucose regulation representing a virtual population with T1DM, the glucose measurement model, and the insulin delivery model. Model parameters were estimated with the maximum likelihood approach for which a prior joint uniform distribution of parameters was determined from glucose measurements in 18 type 1 diabetes patients.

2.2 The Sensor Model

An important component of the simulation environment is the sensor model. The sensor model is used to predict the individuals' sensor glucose profiles based on

their plasma glucose levels. This allows for comprehensive testing of the dosing algorithm, leading ultimately to an accelerated development of the artificial pancreas.

As of now, a few attempts to model the dynamics of CGM have been published, all based on the assumption of one-compartment dynamics between BG and IG [19]. Breton and Kovatchev [20] modeled glucose sensor profiles by a one-compartment model and decomposed sensor error into errors due to calibration, blood-to-interstitial dynamics, and noise. Lunn et al. [21] proposed a more refined model and estimation strategy, which allowed the estimation of model parameters and intra- and interpatient variability simultaneously. Their model accounted for additive and multiplicative multiple calibration errors, and they proposed an autoregressive structure for the measurement error. Facchinetti et al. [22] included a time-varying component to account for sensor drift and used multiple sensors to dissect the sensor error into physiology-related and technology-related.

Owing to mechanical pressure on the sensor site, the sensor reading often experiences sudden temporal unphysiological drops followed by recovery, referred to as drop-outs (see, for example, Fig. 1) (for a detailed review of the physiology of pressure-induced sensor attenuations, we refer the reader elsewhere [23]). In the case of the artificial pancreas, this effect may lead to insulin suspension and, in the dual-hormone system, glucagon delivery, increasing the risk of temporary hyperglycemia. This inspired the development of detection strategies that could be used as part of the artificial pancreas dosing

algorithms[24], [25]. Testing and developing detection and action strategies to mitigate the effect of drop-outs could be facilitated by incorporating drop-out models as part of the in silico simulations. No effort, however, has been made yet to incorporate drop-outs within the sensor dynamical model. In this thesis, we use a probabilistic approach to extend the model of Lunn et al. [21] described above to account for drop-outs and sensor drifts.

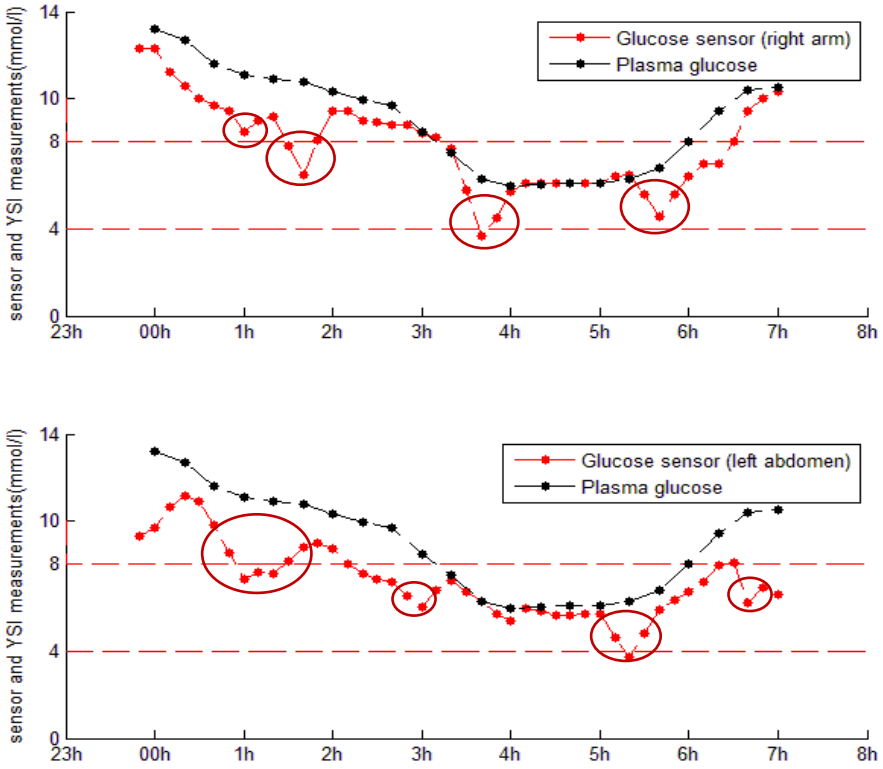

Fig. 2.1: Sensory glucose readings (SG) in red are plotted against plasma glucose (PG; measured by YSI) in black in one subject wearing two sensors. Note the dropouts (marked with red circles).

2.3 Endogenous Glucose Production

Endogenous glucose production (EGP) is a key component of blood glucose regulation; its suppression contributes to the control of post-prandial glucose excursion minimizing hyperglycemia, while its stimulation prevents hypoglycaemia. EGP is mainly controlled by two hormones, insulin and glucagon, and a mathematical model governing its dynamics is an integral part of all simulation environments. Early simulation models [11], [16], [17], [26] included insulin action only, and built on either the minimal model [27], the stable-label two-compartment model [28], or the Hovorka model [1]. These models were useful to test single-hormone closed-loop systems [29] but lacked glucagon action models. Recently, attempts have been made to extend these models to include glucagon action models to allow testing of dual-hormone closed-loop systems. In particular, Herrero et al. proposed a glucagon action extension to the minimal model [30], Markakis et al. proposed a glucagon action extension to the Hovorka model [31], and Hinshaw et al. proposed a model that relates endogenous glucose production with hepatic glucagon sensitivity, and prevailing glucose concentrations [32]. We will detail the features of these models further in Chapter 4.

These glucagon models were proposed as stand-alone and were not compared to potentially superior candidate models. Different models affect simulation results depending on how they characterize the manner in which glucagon levels increase EGP, how glucagon action changes when insulin levels vary, and whether it is the ratio or the absolute levels of glucagon and insulin that affect

EGP, among others. While there are answers put forth addressing some of these issues in human and animal physiology studies [33]–[36], there currently lacks mathematical models developed from real subject data that captures some of these relationships, which is necessary for the simulation environments to reliably test dual-hormone closed-loop systems.

2.4 Technical Background

The models we develop in the chapters that follow will be composed of many parameters that are influenced by a combination of both prior information about the population parameter understood from physiology, and the evidence from information contained in a sample (measurement from data). Bayesian estimation is a method of statistical inference that naturally incorporates these two factors to determine estimations for these parameters.

Let y be the vector representing the measurement, i.e plasma insulin or glucose levels, and θ the vector of unknown parameters.

The likelihood function, $p(y|\theta)$, describes the probability of the observed measurements given the parameter values, θ. Recall Bayes' theorem:

$$p(\theta|y) = \frac{p(y|\theta)p(\theta)}{p(y)} \quad (1)$$

where $p(\theta)$ is the *prior* on θ (which characterizes knowledge about θ before having seen the data), and $p(\theta|y)$ is the posterior density of θ. The estimation problem consists of determining the joint posterior density of all the unknown variables θ conditioned on the observed data. Inference about θ follows from

summarizing the likelihood (for frequentists) or the posterior density (for Bayesians). In the case of uninformative (vague) priors, p(θ) approximates a constant, which renders the posterior density proportional to the likelihood, resulting in the same inference about θ regardless of being in the Bayesian or classical framework.

In Bayesian estimation, inference involves describing features of the posterior distribution of θ, There are several algorithms, both exact and approximate, for carrying out inference in Bayesian estimationIn most cases, inference cannot be performed exactly, leading to the emergence of approximate methods such as Monte Carlo (MCMC) simulation, importance sampling, variational methods, loopy belief propagation, variational inference, or parametric approximation methods. Amongst these approximate methods, Markov Chain Monte Carlo techniques [37] are often favored and seen to perform most efficiently on larger sample sizes. Unlike procedures for conventional statistical inference (i.e, MLEs and least square estimators) that produce point estimates through optimization, these techniques produce samples from the joint posterior density of model parameters that are then summarized for the purpose of inference.

MCMC techniques work by randomly drawing samples from the posterior distribution of the data given the parameters. The Markov chain property of MCMC stems from the idea that a special sequential process governs the generation of the random samples whereby the generation of each random sample depends only on the one before it (hence the “Markov” property).

The sampling mechanism itself obeys a very similar structure: MCMC begins

with an initial guess for the first sample that might be plausibly drawn from the prior distribution. Then, MCMC is used to produce a chain of samples from this initial guess. Each new sample is generated by the following two steps: first, the *proposal* is generated via a small random perturbation to the previous sample; second, this proposal is either accepted as a new sample or rejected (retaining the old sample). There are several different ways of creating the random noise used to generate a proposal, and also several algorithms for the process of accepting/rejecting a proposal, the most popular of which being Gibbs Sampling (used when p(θ | y) is known—parameter values are drawn and kept throughout the chain,) and Metropolis Hastings (used when p(θ | y) is unknown—parameter values are proposed, then either kept or rejected). In our thesis, we employ the method of Metropolis Hastings given that for any parameter we consider, its full conditional distribution is not available in closed form.

The algorithm for Metropolis-Hastings works as follows:

1. Each parameter is assigned an initial value, drawn randomly from its prior distribution, unless the initial value is specified (for the purpose of speeding up the process).
2. A new value is proposed for each model parameter p using some distribution S (often the normal distribution, particularlyN(0,5), for our problem):
$$\theta_p^* \sim S(\theta_p^* | \theta_p)$$
3. The proposed value is then accepted as the current value with probability max(R_{MHG},1):
$$R_{MHG} = \frac{p(y|\theta_p^*)p(\theta_p^*)S(\theta_p|\theta_p^*)}{p(y|\theta_p)p(\theta_p)S(\theta_p^*|\theta_p)}$$
4. The process repeats for a specified number of iterations (until convergence).

For a long enough chain, the final values will represent those drawn from the

posterior distribution (from which the parameter estimates are determined). This is commonly known as convergence. An adaptive phase (or burn-in period) is used where a chain is allowed to run for a set number of iterations (so that the chain may converge) before the sampled parameter values are used to summarize the posterior distribution.

2.5 WinBugs Modelling Framework

The software we used to solve the Bayesian problem, as well as to construct and analyse the models, is WinBugs (Bayesian inference Using Gibbs Sampling) [38], a fully extensible modular framework in which one can construct an internal representation of the probability model in a way that is analogous to the way the model may be visualized graphically. More specifically, each quantity in the model is represented by a node and nodes are connected by arrows to show dependence. The distributional assumptions of each node are 'hidden' to maintain the qualitative nature of the model, and the structure of these dependencies, being directed and without cycles, leads naturally to a directed acyclic representation (DAG) that WinBugs is designed to handle. To deal efficiently with arbitrarily complex models, WinBugs uses object-orientation to represent various nodes in the model. Statistical analysis of the model itself then follows using the Markov chain Monte Carlo simulation methods like those described in the previous section. For more details on the framework and structure of the software, we refer the reader to [38].

CHAPTER 3
Enhancing Glucose Sensor Models: Modelling the Dropouts

3.1 Chapter Contribution

Computer simulation environments have been used in the development of many artificial pancreas systems. A glucose sensor model is an essential part of these environments, and different models have been proposed. However, none of these models account for sudden, temporal unphysiological drop of sensor readings (or better known as “droup-outs”, a well-known phenomenon caused by physical pressure on the sensor site. These dropouts, being unrepresentative of blood glucose level in the subject, may mislead the decisions made by the dosing algorithm in Artificial Pancreas, leading possibly to insulin suspension, increasing the risk of temporary hyperglycemia.

In this chapter, we propose an enhanced model that accounts for drop-outs, and demonstrated its improvement over the existing one-compartment model. Potential drop-outs were augmented to the existing model and their incidences and parameters were estimated with the parameters of the model using the Bayesian approach. Drop-outs and model parameters were estimated from data collected from 15 subjects with type 1 diabetes who underwent an artificial pancreas study. Model fitting and parameter estimates were contrasted between the enhanced model and the one-compartment model. The enhanced model improves fitting of glucose levels and should allow more realistic simulations.

3.2 Subjects and Methods

Model parameters were estimated using data from 15 subjects with type 1 diabetes. Subjects were admitted to a clinical research facility for 15 h, from 16:00 h until 7:00 h the following day. A meal was consumed at 18:00 h and a snack at 22:00 h. Insulin boluses were given with the meal but not the snack. Glucose levels were controlled by insulin and glucagon delivery adjusted every 10 min using a model predictive control algorithm and real-time continuous glucose sensor readings. IG was measured using a Sof-sensor® glucose sensor (Medtronic, Northridge, CA), and plasma glucose was measured using the YSI2300 STAT™ Plus analyzer (YSI, Yellow Springs, OH). The data relevant to this article are the sensor glucose and plasma BG measurements. For more details, we refer the reader to Haidar et al. [39].

3.3 The Model of Lunn et al.

Interstitial glucose (*IG*) is related to the blood glucose (*BG*) by the following first order differential equation:

$$\frac{dIG(t)}{dt} = -k_1 IG(t) + k_2 BG(t) \qquad (1)$$

where k_1 and k_2 are transfer rate parameters. The sensor does not measure *IG* directly but maps an electric current generated in the sensor to a scaled measure of *IG*. Therefore, the sensor uses occasional calibrations (every 8-12 hours) to match electric current values to blood glucose estimates. Normalized interstitial glucose is therefore defined by:

$$\frac{dNIG(t)}{dt} = -k_1[IG(t) - BG(t)] \quad (2)$$

where $NIG = k_1/k_2\ IG$. The calibration process itself is confounded by inaccuracies in the glucose meters. As a result, the dynamical model is characterized after each calibration with its own error parameters, defined m_l (multiplicative error) and e_l (additive error) for $l = 1..C$ calibrations, leading to the following equation:

$$CIG(t) = m_l NIG(t) + e_l \text{ for } l = 1...C \quad (3)$$

where *CIG* denotes "Corrected Interstitial Glucose". Finally, the *i*th sensor glucose measurement is related to *CIG* by

$$SG_i = CIG_i + \in_i, \quad (4)$$

where $\in_i$ is a first order autoregressive process with an autocorrelation of ρ [21].

3.4 Sensor Drop-outs and Drift – The Enhanced Model

To account for sensor drifts, we assumed that the additive errors are time-varying – a special case of the time variability proposed in Facchinetti et al [22]. More specifically, we assumed that the error has a tendency to decrease or increase in time linearly until the next calibration is performed. Accordingly, between two calibrations times, the model now becomes

$$CIG(t) = m_l NIG(t) + e_l + \mathrm{s} \times t, \quad (5)$$

where s determines the extent of error variation over time.

We defined a discrete variable, $isDropout_d$, at every time point d that

takes a value of 0 or 1. If $isDropout_d$ is 1, then glucose levels drop and recover in the next 40 minutes based on the following equations:

$$DropoutFlux_d = -\frac{peakValue_d}{100}t + \frac{d \times peakValue_d}{100}, t \in (d, d+10) \quad (6)$$

$$DropoutFlux_d = \frac{peakValue_d}{100}t + \frac{(d+20) \times peakValue_d}{100}, t \in (d+10, d+30) \quad (7)$$

$$DropoutFlux_d = -\frac{peakValue_d}{100}t + \frac{(d+40) \times peakValue_d}{100}, t \in (d+30, d+40) \quad (8)$$

$$DropoutFlux_d = 0, t \notin (d, d+40) \quad (9)$$

$$TotalDropoutFlux = \sum_d DropoutFlux_d \quad (10)$$

where $peakValue_d$ (mmol/L) determines the nadir of the decline (Figure 3.1, left panel), and t. In the case of overlapping drops (two or more drops that occur within the span of each other's 40 minute durations), the resulting structure would be the addition of the two. This allows the model to manage cases in which the drop-out shape is not the curve specified in the above equations (See for example Figure 3.1, right panel). The $DropoutFlux_d$ values are interpreted as the rate of change of NIG introduced by the dropout effect. Its sum across all time points d, $TotalDropoutFlux$, is incorporated into equation 2 as follows:

$$\frac{dNIG(t)}{dt} = -k_1[IG(t) - BG(t)] + TotalDropoutFlux \quad (11)$$

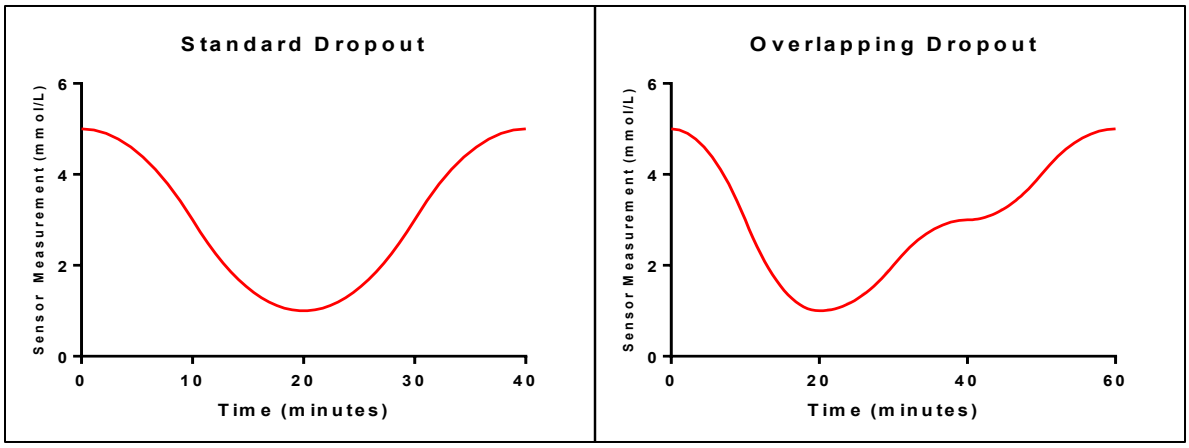

Fig. 3.1: The left graph shows an example of a standard drop-out, as specified by the enhanced model. The duration of the drop-out is 40 minutes, with its peak drop at 20 minutes. Its peak value is 4 mmol/L. The right graph shows an example of an overlapping drop-out.

3.5 Parameter Estimation

We used Bayesian techniques and Markov chain Monte Carlo methods [37] to estimate simultaneously model parameters and the drop-outs. The Bayesian problem was solved using WinBUGS software [38], with WBDiff interface [40] used to allow the specification of the differential equations. Prior distributions of model parameters were set as follows:

$$isDropout_d \sim bernouli(p) \quad (12)$$

$$p \sim uniform(0,1) \quad (13)$$

$$peakValue_d \sim norm(3,1) \quad (14)$$

$$k_1 \sim LN(-2.8, 0.001) \tag{15}$$

$$m_l \sim LN\left(0, \begin{bmatrix} 0.0001 & 0 \\ 0 & 0.0001 \end{bmatrix}\right),\ l = 1..C \tag{16}$$

$$e_l = mnorm\left(0, \begin{bmatrix} 0.0001 & 0 \\ 0 & 0.0001 \end{bmatrix}\right),\ l = 1..C \tag{17}$$

We restricted the drop-out size to be more than 1.5 mmol/L to force the model to use these potential deviations to fit only prominent drop-outs. When no restriction was put on the size of the drop-outs, the model had tendencies to fit other discrepancies between the model and the data, including small non-significant errors, using these potential deviations. The priors specifying the shape and duration of dropouts, including $isDropout_d$ and $peakValue_d$ are set given observations of the data, while the priors for the transfer rate, additive error, and multiplicative error (equations 15-17) are set in accordance with Lunn's model [21].

For the purposes of parameter estimation, measurement errors were assumed correlated and follow a first order autoregressive process with an autocorrelation of ρ:

$$\sigma(i) = (1 - \rho)\sigma(i - 1) + error \tag{18}$$

$$error \sim norm(0, 0.03) \tag{19}$$

Model Comparison

A meaningful way to compare models is to use a criterion based on the trade-off principle of rewarding the model for how well it fits the data while penalizing it for complexity. Based on this principle, Spiegelhalter et al. [41] proposed a Bayesian model comparison criterion, termed the Deviance Information Criterion, and defined as DIC = 'goodness of fit' + 'complexity'. The goodness of fit is captured via the deviance:

$$D(\theta) = -2\log p(y|\theta) \tag{20}$$

Complexity is measured via the estimation of the 'effective number of parameters':

$$p_D = E_{\theta|y}[D] - D(E_{\theta|y}[\theta]) = \overline{D} - D(\bar{\theta}) \tag{21}$$

where $E_{\theta|y}[D]$ is the expected value of $D(\theta)$ given y (posterior mean deviance) and $D(E_{\theta|y}[\theta])$ is the deviance evaluated at the posterior mean of the parameters.

The DIC is then formally defined as:

$$DIC \equiv D(\bar{\theta}) + 2p_D = \overline{D} + p_D \tag{22}$$

We thus define the best performing model as the model with the lowest DIC among the models that have physiologically plausible parameters estimates. By physiologically plausible, we mean that the values are sensible (within an order of magnitude) according to physiological findings, many of which can be found in [1] and [42].

We further use the method of mean weighted residuals to quantify the goodness

of fit of the best performing model [43]. The measure of mean weighted residuals, often summarized as a range of percentages by which the fit deviates from the data, allows for a stand-alone evaluation of any one model's performance.

The enhanced model is contrasted against Lunn's model using the deviance information criterion [41] and weighted residuals. Individual weighted residuals at every time point, *j*, were calculated using:

$$R_i = (CIG_i - SG_i)/\sigma_i^2 \quad (23)$$

where σ_i^2 is the variance of the error of *jth* measurement which is multiplicative with 3% CV.

3.6 Results

Samples of Model Fit

Figure 3.2 shows two sample fits for one individual using Lunn's model and the enhanced model. The Figure shows that dropouts present at times 350 min, 650 min, and 900 min were better fitted with the enhanced model compared to Lunn's model.

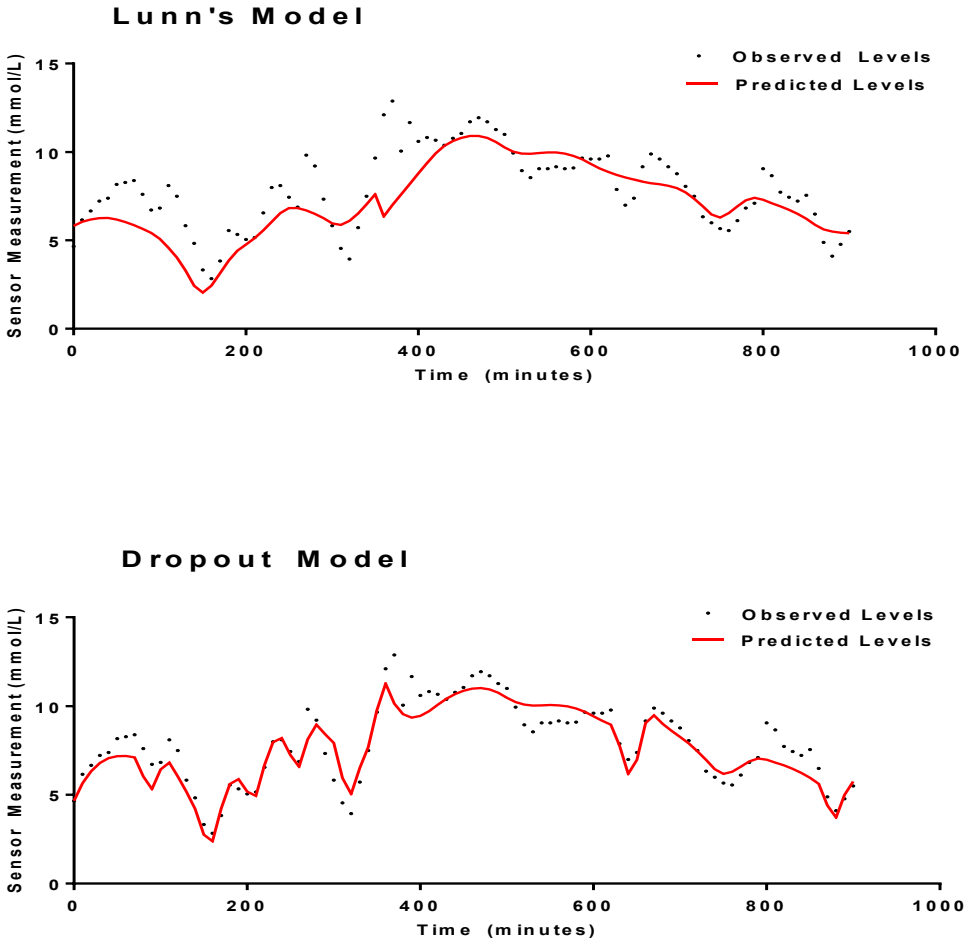

Fig. 3.2: Graphs of model-derived SG (red) plotted against actual subject SG data points (black) for a subject, where the above and bottom graphs are fit using the Lunn's model and the enhanced drop-out model, respectively. Note the inability of Lunn's model to fit for the drop-outs.

Parameter Estimates and Goodness of Fit

Parameter estimates of the two models, including the drop-out parameters for the enhanced model are shown in Table 3.1. Both models achieved similar parameter estimates (p = NS), and all parameters were physiologically plausible. The enhanced model further estimated 1.71 drop-outs per day, which improved model fit (weighted residual reduced from [Min -4%, Max 3%] to [-3%, 2%]; Figure

3.3) and reduced significantly the deviance information criteria from 2739 to 1456.00 (Table 3.1).

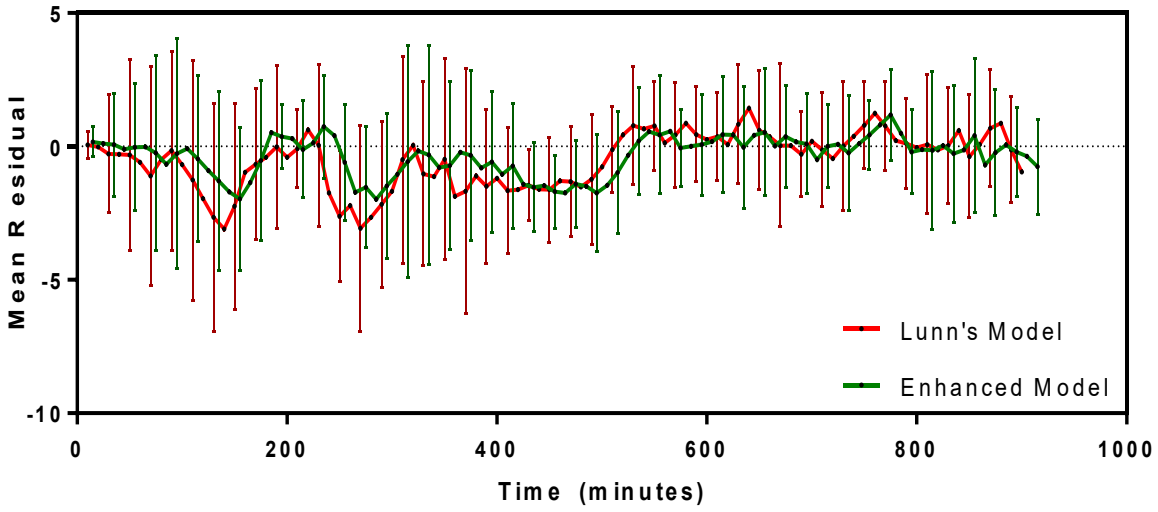

Fig. 3.3: Graph of mean weighted residuals for the previous model's fit (red) and that of the mean weighted residuals for the drop-out model's fit (green), where the vertical axis denotes the mean percent difference between all subjects' sensor glucose readings and those predicted by the model and the horizontal axis is time, in minutes.

Table 3.1. Parameter estimates of the sensor models, with autocorrelation coefficient of the autoregressive error (ρ) assumed 0.7.

Parameter*	Lunn's Model	Enhanced Model	P-value
k_1	0.094 (0.059 – 0.113)	0.110 (0.073 – 0.121)	0.071
m_1	0.920 (0.833 – 1.158)	0.886 (0.833 – 1.055)	0.726
m_2	0.9123 (0.772 – 0.986)	0.888 (0.779 – 0.947)	0.296
e_1	-0.063 (-1.328 – 0.609)	0.035 (-0.054 – 0.101)	0.195
e_2	-0.003 (-0.373 – 0.952)	0.104 (-0.027 – 0.385)	0.664
Number of drop-outs (per subject per experiment)	-	0 (0 – 1.5)	-
Drop-out peak value	-	2.2 (2.086 – 2.395)	-
Frequency of drop-outs (per day)¶	-	1.7	-
Deviance Information Criterion	2739.72	1456.00	-

* Values are median (interquartile range; N=15). Individual point estimates were inferred using medians of posterior realizations

¶ Calculated as the total number of drop-outs (overlapping drop are counted as a single drop-out

Autoregressive Assumption of Model Error

We estimated the parameters of the enhanced model assuming a white noise structure for the model error (e.g, no correlation between consecutive measurement errors). This led to an increase in the number of drop-outs estimated, almost doubling the number from 1.7 to 3.0 drop-outs per day (Table 3.2). Based on visual inspection, the model used drop-outs to fit both real drop-outs and other large discrepancies, resulting from model misspecification, between the model and the data. In other words, the increased rate of drop-outs is a reflection of model misspecification, suggesting, as indicated by others [21], [22], that the autoregressive structure is an attribute of the sensor residual error.

We varied the autocorrelation parameter of the error autoregressive process, ρ, and estimated model parameters and the drop-outs. Similar to what was shown by Lunn et al. [21], model parameters estimated were not sensitive to the value of ρ (Table 3.3).

Table 3.2. Parameter estimates of the drop-out model, without autoregressive structure assumed.

Parameter*	**Drop-out Model**
Number of Drop-outs (per subject per experiment)	1 (0 – 3)
Drop-out Peak Value	2.647 (2.209 – 3.446)
Frequency of Drop-outs (per day) ¶	3.0

*Values are median (interquartile range) (N=15).
¶ Calculated as the total number of drop-outs (overlapping drop are counted as a single drop-out) across all subjects divided by the total number of hours multiplied by 24.

Table 3.3. Parameter estimates of the drop-out model, with autoregressive structure assumed

Parameter*	Drop-out Model (ρ= 0.6)	Drop-out Model (ρ= 0.7)	Drop-out Model (ρ= 0.8)
Number of Drop-outs (Average per subject/per day)	0 (0 – 1.5)	0 (0 – 1.5)	0 (0 – 1.5)
Drop-out Peak Value	2.24 (2.11 – 2.33)	2.2 (2.09 – 2.40)	2.28 (2.09 – 2.68)
Probability of Drop-out (Per hour)	0 (0 – 0.1)	0 (0 – 0.1)	0 (0 – 0.1)
Frequency of drop-outs (per day)	1.6	1.7	1.8

*Values are median (interquartile range) (N=15). Individual point estimates were inferred using medians of posterior realizations.

¶ Calculated as the total number of drop-outs (overlapping drop-outs are counted as a single drop-out) across all subjects divided by the total number of hours multiplied by 24.

3.7 Discussion

We have proposed an enhanced sensor model that takes into account signal drop-out, a frequent phenomenon triggered by physical pressure on the sensor site. We augmented the model presented by Lunn et al [21] to include drop-outs using the Bayesian framework. The new model improved model fit and significantly decreased deviance information criteria. However, the two models predicted similar parameters (sensor delay, calibration errors, etc), suggesting that estimates produced by the previous model remain valid.

The primary purpose for developing sensor models is to use them in metabolic

simulators that test artificial pancreas systems [11]. Although the models proposed by others [20]–[22] seems to provide plausible and valid parameter estimates, they still lack the ability to predict realistic drop-outs during simulations. Drop-outs during artificial pancreas operation might lead to insulin suspension, and in the dual-hormone system, glucagon delivery, increasing the risk of temporary hyperglycemia. Testing and developing strategies to mitigate the effect of drop-outs could be facilitated by drop-out models. Our model estimates frequency and magnitude of drop-outs from real sensor data.

Lunn's model and the enhanced model still display unexplained fluctuations from their fits. Whether or not more sophisticated models can correct for such discrepancies merits further research. Another noteworthy consideration is that we used data measured with the Sof-sensor® glucose sensor. Lunn's model was developed from a different sensor, the Guardian RT CGM system [21]. While the results show that the new model is superior to the old one insofar as modelling the Sof-sensor® glucose sensor, whether or not the new model can be similarly improved for other sensors merits further research.

In summary, we have enhanced the previous model in order to more accurately describe the drop-outs that frequently affect glucose sensor readings. Having proposed a general approach applicable to other sensors, this thesis invites future studies of similar spirit on diverse datasets.

CHAPTER 4
Modelling Glucagon Action in Type 1 Diabetes

4.1 Chapter Contribution

Current simulation environments consider glucose regulation models that either do not include glucagon action sub-models, or include sub-models that were proposed without comparison to other candidate models. In the following chapter, we consider nine candidate models of glucagon action featuring a number of possible characteristics: insulin-independent glucagon action, insulin/glucagon ratio effect on hepatic glucose production, insulin-dependent suppression of glucagon action, and the effect of rate of change of glucagon. To assess the models, we used measurements of plasma insulin, plasma glucagon, and endogenous glucose production collected from experiments involving 8 subjects with type 1 diabetes who received four subcutaneous glucagon boluses. We estimated each model's parameters using a Bayesian approach, and the models were contrasted based on the deviance information criterion. The model achieving the best fit features insulin-dependent suppression of glucagon action and incorporates effects of both glucagon levels and its rate of change.

4.2 Experimental Data

Model parameters were estimated using data collected by El Youssef et al. [44] from 8 subjects with type 1 diabetes who underwent one to three experiments of 8 hours in duration each. On each occasion, they were exposed intravenously to three different insulin infusion rates (low 0.016, medium 0.032, and high 0.05 units/kg/h), and received 4 scheduled subcutaneous glucagon boluses given every

2 hours with different sizes (25, 75, 125, and 175 μg). The first glucagon bolus given was randomized in blocks that followed a chronological order (e.g 75, 125, 175, 25). Insulin (mU/L) and glucagon (pg/mL), were measured every 10 minutes, and EGP levels (umol/kg/min) were calculated using isotope tracer methodology and hierarchical Bayes modeling, as described by Haider et al. [45], [46]. Additionally, 10% dextrose was infused variably in order to maintain constant glucose levels at around 5 mmol/L. In the original study, El Youssef et al. completed twenty-nine occasions in 11 subjects; among these, certain occasions showed a continued rise in glucose infusion rates (implying that the first dose was delivered before steady-state insulin levels were achieved), and very high basal estimates of EGP (i.e., at time 0), likely due to the tracer plasma levels not reaching steady state. For the purpose of our modeling task, we selected only those occasions that did not have these characteristics, which amounted to 13 among the 8 patients, of which 4 had high insulin levels, 5 had medium insulin levels, and 4 had low insulin levels. The occasions that were not used were excluded before any modelling work was conducted.

The mean plasma insulin levels (over 8 hours) for the low, medium, and high insulin infusion rate occasions were 10.1 (9.1-20.4), 28.5 (24.7-36.4), and 40.0 (31.6-44.6) mU/L, respectively. The basal (time 0) plasma glucagon level for the 13 occasions was 83.98 (60.14-151.9) pg/mL. The pre-bolus glucagon levels at the 25, 75, 125, and 175 μg boluses were 147.3(112.5-159.7), 107.1(73.9-134.0), 114.6(97.1-122.9), and 106.5(84.1-152.7) pg/mL, respectively. The peak glucagon level measured after the 25, 75, 125, and 175 μg boluses were

232.2(205.8-287.8), 347.8(333.6-458.9), 506.4 (435.8-700.5), and 640.2 (621.5-785.4) pg/mL, respectively. The mean plasma glucose level across all occasions was 5.2 (4.5-7.8) mmol/L. These characteristics are reported below in Table 4.1.

Table 4.1 Data Characteristics.

	Glucagon Bolus			
Glucagon level (pg/mL)	25µg	75 µg	125 µg	175 µg
Pre-bolus glucagon level	147.3 (112.5-159.7)	107.1 (73.9-134.0)	114.6 (97.1-122.9)	106.5 (84.1-152.7)
Peak glucagon level	232.2 (205.8-287.8)	347.8 (333.6-458.9)	506.4 (435.8-700.5)	640.2 (621.5-785.4)
Basal plasma glucagon level for all occasions				83.98 (60.14-151.9)
	Rate of Insulin during Occasion			
Insulin	Low	Medium	High	
Mean plasma insulin level (8 hours), (mU/L)	10.1 (9.1-20.4)	28.5 (24.7-36.4)	40.0 (31.6-44.6)	
Mean plasma glucose level for all occasions (mmol/L)			5.2 (4.5-7.8)	

4.3 Model Structure

Background

The liver and the kidneys are the main organs responsible for glucose production; 5-20% from the kidneys, and the remaining from the liver [47]. Accordingly, EGP can often be approximated using hepatic glucose production. Endogenous glucose production mainly occurs as a result of two processes: glycogenolysis (breakdown of glycogen to form glucose) and gluconeogenesis

(formation of glucose from smaller molecules). A very important methodological problem in vivo is the dissection of glucose production into its gluconeogenic and glycogenolytic components. Studies indicate that although glucagon and insulin affect the activity of the gluconeogenic pathway within the liver, they have little or no impact on the amount of glucose derived from gluconeogenesis [34], [48]. The metabolic pathway of gluconeogenesis results primarily from substrates such as pyruvate, lactate, glycerol and glucogenic amino acids [42].

The candidate models we propose are motivated by various such physiological findings and developed as sets of equations.

Model 1

Dose-response studies performed on dogs and humans [49] suggest that endogenous glucose production increases steadily with glucagon, eventually saturating at glucagon levels higher than 800 pg/ml. Similarly, dose-response studies for insulin's effect on EGP (example, Holther-Nielsen et al. [36]) demonstrate a steady drop of EGP with insulin, saturating smoothly at insulin levels over 100 μu/ml. The relationships observed seem to indicate that glucagon and insulin effect on EGP can potentially be modeled exponentially. Moreover, Parrilla et al. [50] performed studies on rats to posit that the glucagon:insulin ratio determines EGP and not the absolute concentration of either hormone.

Accordingly, we propose Model 1 as the following equation:

$$EGP(t) = EGP_0 \cdot e^{\frac{-S \cdot X(t)}{T \cdot Gluc(t)}}$$

$$\text{where } \dot{X}(t) = -k \cdot X(t) + k \cdot Ins(t) \qquad (1)$$

where $EGP(t)$ is the projected value for EGP in umol/kg/min, EGP_0 is the EGP at zero insulin levels, *T* is the glucagon sensitivity, *S* is the insulin sensitivity, *Gluc(t)* is the measured glucagon concentration, *X(t)* is the remote insulin concentration, *k* is fractional deactivation rate constant, and *Ins(t)* is the plasma insulin concentration. For the subsequent models, these terms will have the same interpretation.

Model 2

In direct opposition to Parrilla et al.'s finding, Cherrington et al. maintain that although the insulin:glucagon ratio may be a helpful way to appreciate the effects of the endocrine pancreas, any given ratio does not produce a constant effect that is independent of the absolute hormone concentrations present [42]. Model 2 is thus put forth as a modification to Model 1, where it uses two additive exponential terms for each hormone:

$$EGP(t) = EGP_0 \cdot (e^{-S \cdot X(t)} + e^{\frac{-1}{T \cdot Gluc(t)}})$$

$$\text{where } \dot{X}(t) = -k \cdot X(t) + k \cdot Ins(t) \qquad (2)$$

Model 3

The assumption that the exponential terms contribute additively is one that may be problematic in the case where insulin concentrations are high. Steiner et al. [35] demonstrate that when large increases in the infusion rates of insulin and glucagon were brought about simultaneously, the effect of the change in insulin became dominant and glucose production fell. In other words, high insulin concentrations lower the hyperglycemic effect of glucagon, thereby rendering small doses of glucagon ineffective. Model 2 does not entirely capture this

phenomenon (no matter how high $X(t)$ is, the contribution from $e^{\frac{-1}{T\cdot \mathrm{Gluc(t)}}}$ remains just as significant). Accordingly, Model 3 would assume the contributions of the exponentials as multiplicative, which is incidentally able to account for this effect.

The previous models do not account for the contribution of gluconeogenesis on EGP, as described earlier. In Model 3, we introduce a new parameter, Gng, being the effect due to gluconeogenesis independent of insulin or glucagon:

$$EGP(t) = EGP_0 \cdot e^{-S\cdot X(t)} \cdot e^{\frac{-1}{T\cdot Gluc(t)}} + Gng$$

$$\text{where } \dot{X}(t) = -k \cdot X(t) + k \cdot Ins(t) \qquad (3)$$

Models 4 & 5

Particularly in cases where glucagon and insulin doses are under the level at which their effect on EGP saturate, their effect on EGP seems to follow a linear behavior.Consequently, two models can be proposed, one of which relates the contributions of insulin and glucagon additively, and the other multiplicatively:

$$EGP(t) = H(1 - S \cdot X(t)) + (T \cdot Gluc(t)) + Gng \qquad (4)$$

$$EGP(t) = H\big(1 - S \cdot X(t)\big) \cdot \big(T \cdot Gluc(t)\big) + Gng \qquad (5)$$

$$\text{where } \dot{X}(t) = -k \cdot X(t) + k \cdot Ins(t),$$

$$\text{and } H(x) \text{ is the unit step function.}$$

The purpose of the unit step function, $H(x)$, is to ensure that EGP remains positive which may not have otherwise held if $S \cdot \mathrm{X(t)} > 1$.

Hovorka's model, very much like these two models, assumes a linear relationship between insulin and EGP [1]. Specifically, the two glucagon action models in the literature mentioned earlier, Markakis et al.'s extension of

Hovorka's model, and Herrero et al.'s minimal model extension, are proposed in very similar spirit to Model 4, being additive and linear. Herrero's model bears one particular difference with Model 4, in that it assumes a multiplicative dependence on the absolute level of glucose, which, given that in our data glucose levels remain roughly constant, would not be meaningful to include.

Models 6 & 7

Wada et al. [51] have shown that after maintaining elevated glucagon levels (with insulin level fixed at basal rate), EGP rises only initially, but immediately drops thereafter. In other words, with glucagon set at a constant value (rate of change is zero), EGP eventually drops to its initial value. It may then seem possible to account for this phenomenon by modelling EGP as a function of rate of change of glucagon instead of its absolute level. Therefore we consider the following two variants:

$$EGP(t) = H(1 - S \cdot X(t)) + H\left(EGP_{Gluc(t)}\right) + Gng \tag{6}$$

$$EGP(t) = H(1 - S \cdot X(t)) \cdot H\left(EGP_{Gluc(t)}\right) + Gng \tag{7}$$

where $\dot{EGP}_{Gluc(t)} = -J \cdot EGP_{Gluc(t)} + T \cdot \left(\frac{dGluc(t)}{dt}\right)$

$$\dot{X}(t) = -k \cdot X(t) + k \cdot Ins(t)$$

$H(x)$ is the unit step function.

Here, $EGP_{Gluc(t)}$ is interpreted as the contribution to EGP from the rate of change of glucagon. It is described in the differential equation as being an exponential decline when rate of change of glucagon is absent, with the decline

counteracted (and possibly reversed) when there is a rate of change. If the rate of change is negative, the decline would be sharpened. However, using the unit step function, $EGP_{Gluc(t)}$ is only allowed to play a positive contribution on EGP.

Model 8

This model augments model 7 by including a contribution from the glucagon level as well as that of its rate of change; this is, of course, in consideration to the general understanding that the amount of glucagon distributed does, after all, affect EGP [33], [52]–[54].

$$EGP(t) = H(1 - S \cdot X(t)) \cdot H\left(EGP_{Gluc(t)} + T \cdot \ Gluc_t\right) + Gng \tag{8}$$

$$\text{where } \dot{EGP_{Gluc(t)}} = \ -k_{Gd} \cdot EGP_{Gluc(t)} - k_{Gd} T_{Gd} \cdot \left(\frac{dGluc(t)}{dt}\right),$$

$$\dot{X(t)} = -k \cdot X(t) + k \cdot Ins_{t,}$$

$$H(x) \text{ is the unit step function.}$$

The parameters for each model, in units, are shown in Table 4.2.

Model 9

Hinshaw et al propose a model [32] describing glucagon action on EGP. Briefly, the dephosporylation of glucose-6-phosphate is assumed to govern EGP:

$$EGP(t) = a \cdot G6P(t) \tag{9}$$

Here, *a* is the dephosporylation rate, and G6P is the dynamics in the liver which is modeled by a first order differential equation:

$$\dot{G6P} = -a \cdot G6P + Glys + Gng, \tag{10}$$

$$where\ G6P(0) = \frac{EGP_b}{a} + g6p0$$

Here, *Glys* is the rate of glycogenolysis (which is further modeled to be linearly dependent on glucagon concentration above a given level, and modulated by an "evanescence effect), *Gng* the rate of gluconeogenesis, EGP_b the basal EGP, and *g6p0* a free parameter accounting for the sudden rise of EGP when glucagon rises above a given level.

This model can incorporate the effect of insulin in a multiplicative way, as follows:

$$EGP(t) = H(1 - S \cdot X(t)) + \ a \cdot G6P(t) \qquad (11)$$

where $H(x)$ is the unit step function

4.4 Parameter Estimation

We used Bayesian estimation in order to estimate model parameters. Markov Chain Monte Carlo methods [37] were exploited in order to produce a posterior joint distribution from which samples can be obtained. The median of these samples were used as a point estimate of parameter estimates.

Implementation Details

The differential equations describing the models were solved numerically using initial conditions, plasma insulin and glucagon levels, and model parameters. MCMC was implemented using WinBUGS version 1.4 [38], with WBDiff interface [40] to numerically solve the differential equations. Prior distributions of parameters for our models were set using estimates derived in the literature [1], [42] . Measurement errors were assumed to be normally distributed with zero mean. The measurement errors associated with EGP were assumed to have a coefficient of variation (CV) of 3%.

Table 4.2 Parameters, units of measurement, and previous estimate for each model

Model	Parameters to be Estimated							
	EGP_0	GnG	k	S	T	T_{Gi}	k_{Gi}
1	$\mu mol/kg \cdot min$	-	min^{-1}	$\frac{mU/L}{mL \cdot \mu mol}$	$\frac{mL/pg}{kg \cdot pg \cdot min}$	-	-
2	$\mu mol/kg \cdot min$	-	min^{-1}	$\frac{mU/L}{mL \cdot \mu mol}$	$\frac{mL/pg}{kg \cdot pg \cdot min}$	-	-
3	$\mu mol/kg \cdot min$	$\mu mol/kg \cdot min$	min^{-1}	$\frac{mU/L}{mL \cdot \mu mol}$	$\frac{mL/pg}{kg \cdot pg \cdot min}$	-	-
4	-	$\mu mol/kg \cdot min$	min^{-1}	$\frac{mL \cdot \mu mol}{kg \cdot pg \cdot min}$	$\frac{mL \cdot \mu mol}{kg \cdot pg \cdot min}$	-	-
5	-	$\mu mol/kg \cdot min$	min^{-1}	$\frac{mU/L}{mL \cdot \mu mol}$	$\frac{mL \cdot \mu mol}{kg \cdot pg \cdot min}$	-	-
6	-	$\mu mol/kg \cdot min$	min^{-1}	$\frac{mL \cdot \mu mol}{kg \cdot pg}$	$\frac{mL \cdot \mu mol}{kg \cdot pg}$	-	-
7	-	$\mu mol/kg \cdot min$	min^{-1}	$\frac{mU/L}{mL \cdot \mu mol}$	$\frac{mL \cdot \mu mol}{kg \cdot pg}$	-	-
8	-	$\mu mol/kg \cdot min$	min^{-1}	$\frac{mU/L}{kg \cdot pg}$	$\frac{mL \cdot \mu mol}{kg \cdot pg \cdot min}$	$\frac{mL \cdot \mu mol}{kg \cdot pg}$	min^{-1}
9	$\mu mol/kg \cdot min$		min^{-1}	$\frac{mU/L}{kg \cdot pg}$			
Expectation:	Positive, previous average finding: 16.1 [1]	Positive, Previous average finding: ~5 [45]	Positive, previous average finding: 0.06 [1]	Positive, previous average finding for $\frac{mU/L}{kg \cdot pg}$: 0.11 [1]	Positive, no previous finding	Positive, no previous finding	Positive, no previous finding

Model Comparison

We define the best performing model as the model with the lowest DIC among the models that have physiologically plausible parameters estimates. For example, insulin and glucagon sensitivity have to be positive, transfer rate parameter for insulin kinetics has to be between 0 and 30 min (3 hr would be non

plausible). Refer back to Table 4.2 for the complete plausibility expectations of the parameters in question.

We further use the method of mean weighted residuals to quantify the goodness of fit of the best performing model [43].. Individual weighted residuals at every time point, *i*, were calculated using:

$$R_i = (EGPp_i - EGP_i)/\sigma_i^2 \quad (12)$$

where $EGPp_i$ is the model predicted EGP for the *ith* measurement, EGP_i is the measured EGP at the *ith* measurement, and σ_i^2 is the variance of the error of *ith* measurement which we assume is multiplicative with 3% CV.

4.5 Results

Parameter estimates of the models are shown in Table 4.3. The parameters for six of the models (1, 2, 5, 7, 8, and 9) were physiologically plausible while those of three of the models (3, 4, and 6) were not. For Model 3, the parameter estimates of EGP_0 were largely non physiological (the estimates varied to many orders of magnitude, with CV exceeding 100%), and Model 4's and 6's (additive models) parameter estimates for insulin sensitivity (*T)* were not plausible with respect to insulin concentrations during occasions in which insulin level is high. This reveals a critical drawback of additive models, as we will discuss in further detail in the next section.

Among the models whose parameter estimates were physiologically plausible and posteriorly identifiable, Model 1, structured as an exponential ratio between insulin and glucagon, showed the highest deviance information criterion (i.e.,

worst performance). Its variant, Model 2, reduced the DIC by 22273 (from 67527 to 45255) simply by separating the effects of insulin and glucagon. Model 5, being the linear counterpart to the previous models, assumed a significant contribution from the gluconeogenesis term, at 5.4 (3.7-8.6), but did not reduce the deviance information criterion compared to Model 2; its DIC was higher by 10463 (53003 vs 45255). Model 7, having also a linear structure, reduced the DIC by replacing the absolute level of glucagon with its rate of change to capture the observed effect of vanishing glucagon effect when its level is constant. Model 8, which incorporates both the absolute concentration of glucagon and the rate of change, significantly reduces the DIC compared to the previous models. Model 9, a re-implementation of Hinshaw et al.'s glucagon action model extended to incorporate the effect of insulin, had a DIC competitive with the previous models (47627) but one that was still significantly higher than Model 8's. As a result, Model 8's DIC demonstrates that EGP can be modeled best in terms of a product of a linear estimation of EGP due to insulin and both glucagon level and rate of change of glucagon. Additionally, all of its parameters were identified with good precision (CV < %100). The mean weighted residuals of Model 8 are shown in Figure 4.2.

Table 4.3: Parameter Estimates for Each Model

Model	*Parameters*					DIC	Plausibility
	EGP_0	Gng	k	S	T/ T_{ad}/k_{ad}		
1	17.0(12.1-31.7)	--	0.084(0.034-0.370)	0.21 (0.14-0.36)	0.13 (0.062-0.24)	67527	Yes
	54.0(31.7-194.0)	--	0.047 (0.023-0.198)	0.095 (0.053 -0.38)	0.0012 (0.00084-0.028)	45255	Yes
3	4895 (2681-30020)	5.243 (2.219-7.442)	0.040 (0.017-0.054)	0.16 (0.13-0.24)	0.0021(0.00091-0.012)	42540	No
4	--	6.44 (2.37-9.02)	0.12 (0.057-0.19)	0.040 (0.034-0.082)	0.022 (0.012-0.034)	59340	No
5	--	5.39 (3.72-8.63)	0.064 (0.028-0.260)	0.034 (0.026-0.039)	0.40 (0.22-0.62)	53003	Yes
6	--	5.43(3.62-7.69)	0.11 (0.022-0.51)	0.11 (0.010-0.32)	0.0016 (0.00065-0.011)	44242	No
7	--	7.54 (6.99-8.23)	0.071 (0.027-0.156)	0.0050 (0.0015-0.034)	0.061 (0.040-0.19)	45716	Yes
8	--	5.54 (5.23-5.98)	0.068(0.027-0.161)	0.020 (0.10-0.036)	0.063(0.020-0.21)	36165	Yes
9	--	8.8 (7.6-9.5)	0.38 (0.32-0.49)	1.1 (1.06-1.16)	T_{ad}: 0.070 (0.026-0.13) k_{ad}: 0.022 (0.021-0.023) --	47627	No

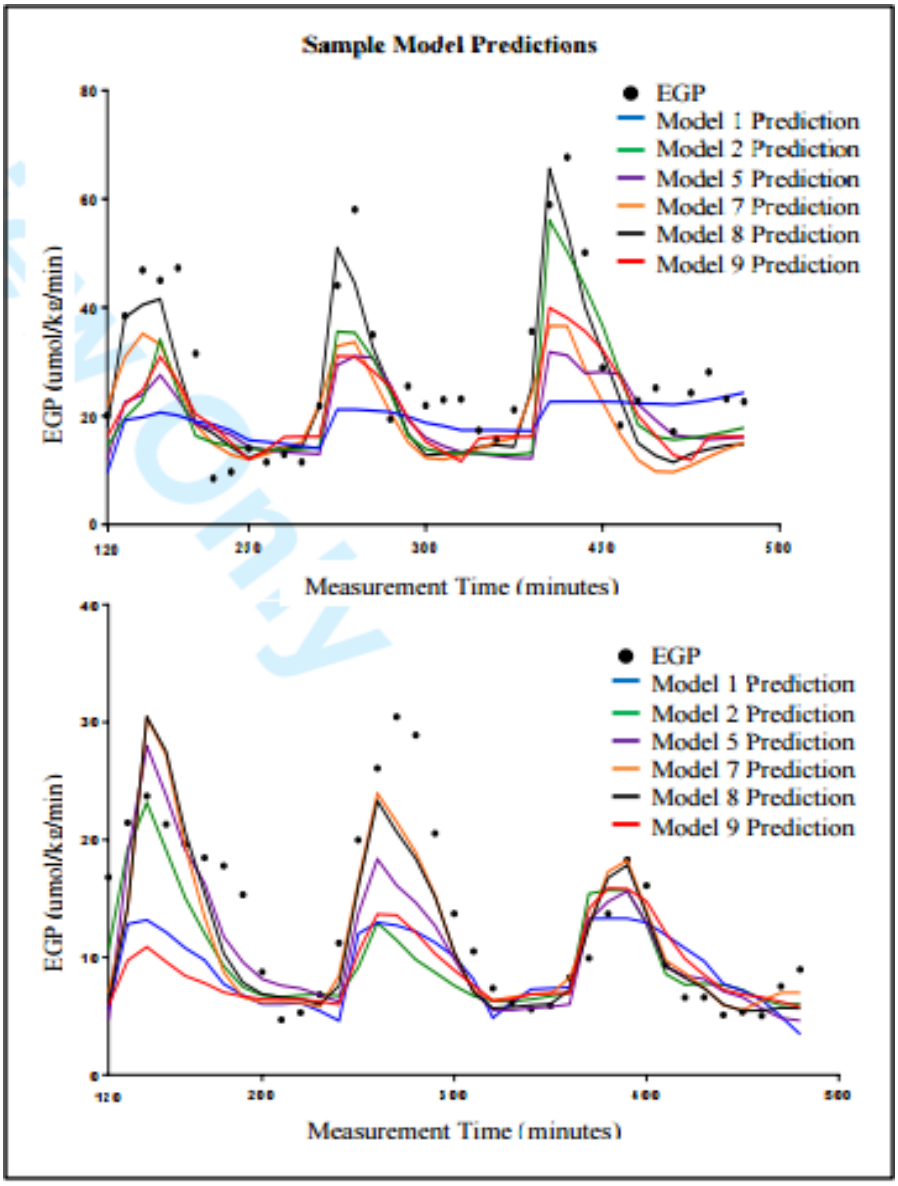

Fig. 4.1: Graph of model fits on two sample occasions. Only models with physiological parameter estimates shown.

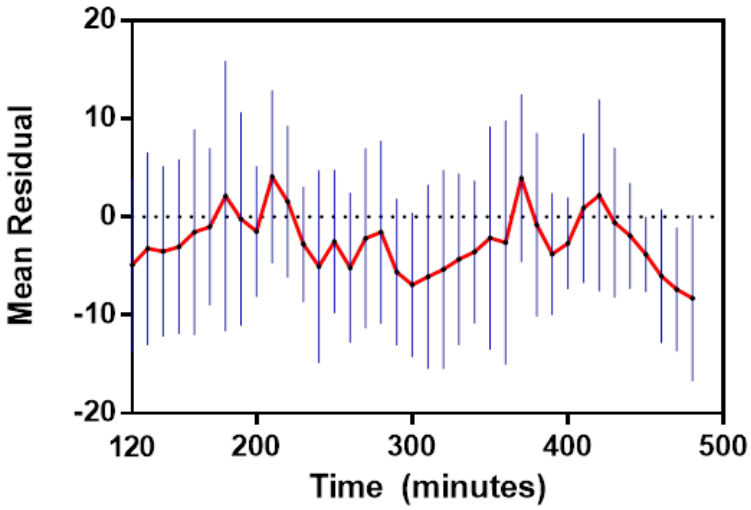

Fig. 4.2: Graph of mean weighted residuals for model 8's fit

4.6 Discussion

Mathematical models for EGP play an important part of in-silico simulations that test closed-loop systems. Particularly, a model that can incorporate the effect of both glucagon and insulin allows the simulations of dual-hormone closed-loop systems. It may also open new horizons for designing clinical studies such as those assessing novel usage of glucagon (e.g., mini dosages to prevent hypoglycemia in an open- or closed-loop manner). In this work, we have proposed a new set of such models, and have compared them on the basis of their deviance information criterion and physiological plausibility.

The first three models assume an exponential relationship between EGP and insulin and glucagon, with varying structures. Model 1 assumes a direct ratio between insulin and glucagon levels to affect EGP, while Model 2 separates the two effects additively, and Model 3 separates them multiplicatively and incorporates an extra term for the contribution of gluconeogenesis. The remaining five models are linear and vary on the basis of additive vs. multiplicative structure and on which factor among absolute level and/or rate of change of glucagon. Models 4 and 5 are the additive and multiplicative linear counterparts to Model 3; they also separate the effects of insulin and glucagon and assume an independent contribution from gluconeogenesis. In order to ensure that the contribution from insulin is positive, the step function was used to prevent the component from being negative. Models 6 and 7 are additive and multiplicative variants to the previous two models, where, instead of considering the absolute level of glucagon as a direct effect on EGP, its rate of change

becomes the key player. In Model 8, we explicitly allowed both the absolute level and rate of change of glucagon to play significant and independent roles in the determination of EGP, along with absolute level of insulin. Finally, Model 9 was developed in a similar spirit to one proposed in the literature [29]. Having tested several different candidate models and various configurations, our Model 8 emerged as the most suitable for our experimental data.

Our models provide several key findings that confirm experimental-based investigations. Model 1's inadequacy compared to the subsequent models suggest the conclusion indicated by Cherrington et al. [42] that the interaction between insulin and glucagon on EGP may not in fact be described as a ratio between the two. The importance of considering gluconeogenesis (a process independent from insulin and glucagon levels) as an effect on EGP is also supported in the models; this is evidenced by the improvement of DIC amongst Models 3, 5, 7, and 8 when the gluconeogenesis term is included. These results could be of great use in dual-hormone closed-loop systems for which the distribution of glucagon is used to counterbalance insulin infusion and prevent hypoglycemia.

We have chosen to estimate parameters using the Bayesian approach as it provides a convenient and natural way of combining prior information (for example, on parameters S, T, and k) with data. Accordingly, it allows what is already expected about the parameters from previous findings to influence the estimation. Markov Chain Monte Carlo methods are a class of computational algorithms to produce posterior joint distributions for the parameters. These

methods are used as closed-loop analytical solution rarely exist for Bayesian problems.

A particularly important finding involves the comparison between additive and multiplicative models. The former, while often favored for their simplicity [10], [30], [31], [55], yield implausible parameter estimates in cases such as our own. In our case, Models 4 and 6, being the additive counterpart of Models 5 and 7, yielded non-physiological parameter estimates. Specifically, during high insulin occasions where glucagon lost its effectiveness [56], the additive models estimated implausible low glucagon sensitivities in order to fit the data (the data indicate no glucagon action despite high plasma glucagon levels, which cannot be fit with non-zero glucagon sensitivities, see equations 4 and 6). This is because, having treated the effects due to insulin and glucagon *independently*, additive models indicate that glucagon acts without restriction regardless of how high or low insulin levels are. In the multiplicative models, however, high insulin levels would directly suppress the effect of glucagon via the model structure (equations 5 and 7) without forcing glucagon sensitivity estimates to be implausible. Consequently, additive models might mislead closed-loop simulations; if used at high insulin levels, glucagon will be considered to have an effect in simulations, which will not be consistent with reality. Accordingly, we present our best model as a multiplicative relationship between insulin and glucagon.

In the design of dual-hormone closed-loop dosing algorithms, two approaches may be used. Either a) using doses of glucagon as a rescue from hypoglycemia

in cases where hypoglycemia occurs despite insulin suspension, or b) allowing more aggressive insulin infusion to further reduce mean glucose levels while using glucagon as a modulator to prevent increasing the risk of hypoglycemia. Our proposed model may aid, via computer simulations or as part of the closed-loop control algorithm, in determining the amount of glucagon required to counteract the insulin effect and to fine-tune the thresholds of insulin infusion levels at which glucagon dosages becomes less effective. In addition, concerning the second approach, simulations could also allow us to determine to what extent we can increase the aggressiveness of insulin delivery without increasing the risk of hypoglycemia due to glucagon inefficacy.

CHAPTER 5
Conclusion

5.1 Discussion

Recent years have seen rapid progress towards the development of closed-loop delivery stems, a new technology to treat type 1 diabetes. An important step in this direction is the completion of simulation environments used to evaluate and test the dosing algorithm central to these systems. In this thesis, statistical modelling techniques and computational methods have been used to develop two models that contribute to the completion of the simulation environments.

In Chapter 3 we propose a sensor model that enhances a previous model in order to more accurately describe the drop-outs that frequent glucose sensor readings. Using a set of differential equations representing the dropout fluxes, the general shape of a single dropout as observed in the data (a parabolic dip in sensory glucose reading of a duration 40 minutes) is mimicked, and its occurrence within a simulated study is governed by a random variable, *isDropout*, along with an attribute *peakValue* (the peak of the dropout dip). In order to account for less-standard shapes and the possibility of overlapping dropouts, the dropout fluxes can be added, resulting in various, less standard shapes. We have shown, then, that a model that incorporates this feature improves model fit and significantly decreased deviance information criteria from that of previous models.

In Chapter 4 a set of physiologically motivated candidate models were used to determine a glucagon action sub model achieving the best fit with the data,

featuring insulin-dependent suppression of glucagon action and incorporating effects of both glucagon levels and its rate of change. Models that incorporated various combinations of these features, at various structures (additive and multiplicative) were proposed and compared.

The important conclusions that emerge from these two models determined in this thesis include the efficacy of accounting for sensor eccentricities for simulation environments, the inadequacy of additive models for certain modelling tasks , as well the clinical significance of the best glucagon action sub-model.

To determine model parameters in both modelling tasks, Bayesian estimation and Markov Chain Monte Carlo methods were used. These methods are becoming increasingly popular as techniques for modelling various systems in a wide variety of domains, including computational biology, our own domain, as well as computational physics, and computational linguistics.

One of the important features of Bayesian estimation is that it allows for the analysis and use of smaller data sets which would otherwise lead to power issues using classical frequentist frameworks [57]. This becomes particularly important when a simulation study or environment is being produced from a naturally small clinical sample, as was precisely the case with the modelling tasks in this thesis.

The combination of the statistical methods of Markov Chain Monte Carlo and the use of the WinBUGS software to specify models and efficiently carry out

the parameter estimation serves as a comprehensive example of their potential use in the development of other novel intervention therapies.

5.2 Limitations of Work

The data we used for our study suffers from certain limitations. For both the sensor and the EGP modelling tasks, the data was taken from other closed-loop studies, and despite having statistical significance in most endpoints, a limitation of the study was its small sample size. In the case of the data used for the EGP models, given that glucose levels were unvarying, we were unable to explore the possible effect of glucose levels on EGP. Nevertheless, our best model's ability to fit the data suggests that EGP may be modelled without the need to consider absolute glucose levels, which is in agreement with recent data in type 1 diabetes [32], unlike what is shown for dogs [58]. It should be mentioned, however, that the recent data only considered EGP during hypoglycemia and euglycemia. It would be the subject of further research to investigate whether this assumption would hold for models during hyperglycemia. Another limitation of the data we used is that it reflects a suppressed endogenous glucagon release (through octreotide) that may not hold in actual applications. To explore more models that would fit for these more realistic situations also merits research. Ultimately, an important first step for the development of such models would be towards preparing richer and more accurate data—both by conducting studies with a larger sample size and by applying more varied protocols involving glucagon and insulin infusion (i.e varying more frequently and markedly the insulin infusion rates). Having

explored the fitting ability and plausibility of a set of candidate models, our work introduces the opportunity to validate the models, which would be another meaningful subject of research.

5.3 Future Work

An important question is whether or not modelling for within-patient and between-patient variability will improve the simulation environment. Within-patient factors including stress, time of day, and level of activity, as well as between-patient variability may result in a change of parameters including glucagon and insulin sensitivity. Quantifying these variabilities during closed-loop operation and their potential relationship with common clinical and demographics variables might improve the performance of closed loop systems and the accuracy of computer simulation environments.

Another important area of research is whether or not a subject's activity level (rest, exercise, etc.) affects sensor performance. Despite technological advances, the accuracy of continuous glucose monitoring (CGM) systems may not always be satisfactory with rapidly changing glucose levels, as is notable during exercise. It would be meaningful to evaluate and compare current sensors during both rest and exercise, in adults with type 1 diabetes. The results would suggest enhancements (such as the dropout enhancement in chapter 2) for the simulation environments that would increase realism. We have preliminary results in this direction accepted for publication in the journal of Diabetes Therapeutics and Technology.

Despite the potential for dual hormone closed loop systems to further prevent hypoglycemic events compared to single hormone closed loop systems [59], the benefits remain to be quantified as the dual hormone closed loop systems are confounded with increased cost and complexity. Randomized trials should be conducted with head to head comparisons between single and dual closed loops systems.

References

[1] R. Hovorka, F. Shojaee-Moradie, P. V Carroll, L. J. Chassin, I. J. Gowrie, N. C. Jackson, R. S. Tudor, A. M. Umpleby, and R. H. Jones, "Partitioning glucose distribution/transport, disposal, and endogenous production during IVGTT.," *Am. J. Physiol. Endocrinol. Metab.*, vol. 282, no. 5, pp. E992–1007, May 2002.

[2] J. A. Todd, "Etiology of type 1 diabetes.," *Immunity*, vol. 32, no. 4, pp. 457–67, Apr. 2010.

[3] D. R. Whiting, L. Guariguata, C. Weil, and J. Shaw, "IDF diabetes atlas: global estimates of the prevalence of diabetes for 2011 and 2030.," *Diabetes Res. Clin. Pract.*, vol. 94, no. 3, pp. 311–21, Dec. 2011.

[4] The Diabetes Control and Complications Trial Research Group, "The effect of intensive treatment of diabetes on the development and progression of long-term complications in insulin-dependent diabetes mellitus," *N Engl J Med*, vol. 329, pp. 977–986, 1993.

[5] J. C. Pickup, H. Keen, J. A. Parsons, and K. G. Alberti, "Continuous subcutaneous insulin infusion: an approach to achieving normoglycaemia.," *BMJ*, vol. 1, no. 6107, pp. 204–207, Jan. 1978.

[6] J. C. Pickup, "Management of diabetes mellitus: is the pump mightier than the pen?," *Nat. Rev. Endocrinol.*, vol. 8, no. 7, pp. 425–33, Jul. 2012.

[7] D. J. Wexler, J. B. Meigs, E. Cagliero, D. M. Nathan, and R. W. Grant, "Prevalence of hyper- and hypoglycemia among inpatients with diabetes: a national survey of 44 U.S. hospitals.," *Diabetes Care*, vol. 30, no. 2, pp. 367–9, Feb. 2007.

[8] H. B. Mortensen, "Findings from the Hvidore Study Group on Childhood Diabetes: Metabolic control and quality of life," *Horm. Res.*, vol. 57, no. SUPPL. 1, pp. 117–120, 2002.

[9] D. L. Longo and P. E. Cryer, "Mechanisms of Hypoglycemia-Associated Autonomic Failure in Diabetes," *N. Engl. J. Med.*, vol. 369, no. 4, pp. 362–372, Jul. 2013.

[10] C. D. Man, F. Micheletto, D. Lv, M. Breton, B. Kovatchev, and C. Cobelli, "The UVA/PADOVA Type 1 Diabetes Simulator: New Features.," *J. Diabetes Sci. Technol.*, vol. 8, no. 1, pp. 26–34, Jan. 2014.

[11] M. E. Wilinska, L. J. Chassin, C. L. Acerini, J. M. Allen, D. B. Dunger, and R. Hovorka, "Simulation environment to evaluate closed-loop insulin delivery systems in type 1 diabetes.," *J. Diabetes Sci. Technol.*, vol. 4, no. 1, pp. 132–44, 2010.

[12] A. Haidar, M. E. Wilinska, J. A. Graveston, and R. Hovorka, "Stochastic virtual population of subjects with type 1 diabetes for the assessment of closed-loop glucose controllers," *IEEE Trans. Biomed. Eng.*, vol. 60, no. 12, pp. 3524–3533, 2013.

[13] E. Moberg, M. Kollind, P.-E. Lins, and U. Adamson, “Day-to-day Variation of Insulin Sensitivity in Patients with Type 1 Diabetes: Role of Gender and Menstrual Cycle,” *Diabet. Med.*, vol. 12, no. 3, pp. 224–228, Mar. 1995.

[14] A. Emami, R. Rabasa-Lhoret, and A. Haidar, “Enhancing Glucose Sensor Models: Modeling the Drop-Outs,” *Diabetes Technol. Ther.*, May 2015.

[15] A. Emami, J. El Youssef, R. Rabasa-Lhoret, J. Pineau, J. Castle, and A. Haidar, “Modelling Glucagon Action in Patients with Type 1 Diabetes,” *IEEE J. Biomed. Heal. Informatics*, vol. PP, no. 99, pp. 1–1, 2016.

[16] S. Kanderian, Steil, and G. Steil, “Identification of Intraday Metabolic Profiles during Closed-Loop Glucose Control in Individuals with Type 1 Diabetes,” 2009.

[17] B. P. Kovatchev, M. Breton, C. D. Man, and C. Cobelli, “In silico preclinical trials: a proof of concept in closed-loop control of type 1 diabetes,” *J. Diabetes Sci. Technol.*, vol. 3, no. 1, pp. 44–55, 2009.

[18] R. Bergman, Y. Ider, C. Bowden, and C. Cobelli, “Quantitative estimation of insulin sensitivity,” *Am J Physiol Endocrinol Metab*, vol. 236, no. 6, pp. E667–677, Jun. 1979.

[19] K. Rebrin, G. M. Steil, W. P. van Antwerp, and J. J. Mastrototaro, “Subcutaneous glucose predicts plasma glucose independent of insulin:

implications for continuous monitoring," *Am J Physiol Endocrinol Metab*, vol. 277, no. 3, pp. E561–571, Sep. 1999.

[20] M. Breton and B. Kovatchev, "Analysis, Modeling, and Simulation of the Accuracy of Continuous Glucose Sensors," *J. Diabetes Sci. Technol.*, vol. 2, no. 5, pp. 853–862, Sep. 2008.

[21] D. J. Lunn, C. Wei, and R. Hovorka, "Fitting dynamic models with forcing functions: application to continuous glucose monitoring in insulin therapy.," *Stat. Med.*, vol. 30, no. 18, pp. 2234–50, Aug. 2011.

[22] A. Facchinetti, S. Del Favero, G. Sparacino, J. R. Castle, W. K. Ward, and C. Cobelli, "Modeling the glucose sensor error.," *IEEE Trans. Biomed. Eng.*, vol. 61, no. 3, pp. 620–9, Mar. 2014.

[23] K. L. Helton, B. D. Ratner, and N. A. Wisniewski, "Biomechanics of the Sensor-Tissue Interface--Effects of Motion, Pressure, and Design on Sensor Performance and the Foreign Body Response--Part I: Theoretical Framework," *J. Diabetes Sci. Technol.*, vol. 5, no. 3, pp. 632–646, May 2011.

[24] N. Baysal, F. Cameron, B. A. Buckingham, D. M. Wilson, H. P. Chase, D. M. Maahs, and B. W. Bequette, "A novel method to detect pressure-induced sensor attenuations (PISA) in an artificial pancreas.," *J. Diabetes Sci. Technol.*, vol. 8, no. 6, pp. 1091–6, Nov. 2014.

[25] B. W. Bequette, "Fault detection and safety in closed-loop artificial

pancreas systems.," *J. Diabetes Sci. Technol.*, vol. 8, no. 6, pp. 1204–14, Nov. 2014.

[26] P. G. Fabietti, V. Canonico, M. O. Federici, M. M. Benedetti, and E. Sarti, "Control oriented model of insulin and glucose dynamics in type 1 diabetics.," *Med. Biol. Eng. Comput.*, vol. 44, no. 1–2, pp. 69–78, 2006.

[27] R. N. Bergman, "Toward physiological understanding of glucose tolerance. Minimal-model approach," *Diabetes*, vol. 38, no. 12. pp. 1512–1527, 1989.

[28] P. Vicini, A. Caumo, and C. Cobelli, "The hot IVGTT two-compartment minimal model: indexes of glucose effectiveness and insulin sensitivity.," *Am. J. Physiol.*, vol. 273, no. 5 Pt 1, pp. E1024–E1032, 1997.

[29] M. E. Wilinska, E. S. Budiman, M. B. Taub, D. Elleri, J. M. Allen, C. L. Acerini, D. B. Dunger, and R. Hovorka, "Overnight closed-loop insulin delivery with model predictive control: assessment of hypoglycemia and hyperglycemia risk using simulation studies.," *J. diabetes Sci. Technol.*, vol. 3, no. 5, pp. 1109–1120, 2009.

[30] P. Herrero, P. Georgiou, N. Oliver, M. Reddy, D. Johnston, and C. Toumazou, "A composite model of glucagon-glucose dynamics for in silico testing of bihormonal glucose controllers.," *J. Diabetes Sci. Technol.*, vol. 7, no. 4, pp. 941–51, Jul. 2013.

[31] M. G. Markakis, G. D. Mitsis, and V. Z. Marmarelis, “Computational study of an augmented minimal model for glycaemia control.,” *Conf. Proc. ... Annu. Int. Conf. IEEE Eng. Med. Biol. Soc. IEEE Eng. Med. Biol. Soc. Annu. Conf.*, vol. 2008, pp. 5445–8, Jan. 2008.

[32] L. Hinshaw, A. Mallad, C. Dalla Man, R. Basu, C. Cobelli, R. E. Carter, Y. C. Kudva, and A. Basu, “Glucagon sensitivity and clearance in type 1 diabetes: insights from in vivo and in silico experiments.,” *Am. J. Physiol. Endocrinol. Metab.*, vol. 309, no. 5, pp. E474–86, Sep. 2015.

[33] P. Felig, J. Wahren, and R. Hendler, “Influence of physiologic hyperglucagonemia on basal and insulin-inhibited splanchnic glucose output in normal man.,” *J. Clin. Invest.*, vol. 58, no. 3, pp. 761–5, Sep. 1976.

[34] J. E. Liljenquist, G. L. Mueller, A. D. Cherrington, U. Keller, Chiasson J-L, J. M. Perry, W. W. Lacy, and D. Rabinowitz, “Evidence for an important role of glucagon in the regulation of hepatic glucose production in normal man.,” *J. Clin. Invest.*, vol. 59, no. 2, pp. 369–74, Feb. 1977.

[35] K. E. Steiner, P. E. Williams, W. W. Lacy, and A. D. Cherrington, “Effects of insulin on glucagon-stimulated glucose production in the conscious dog.,” *Metabolism.*, vol. 39, no. 12, pp. 1325–33, Dec. 1990.

[36] O. Hother-Nielsen, J. E. Henriksen, J. J. Holst, and H. Beck-Nielsen, “Effects of insulin on glucose turnover rates in vivo: isotope dilution

versus constant specific activity technique.," *Metabolism.*, vol. 45, no. 1, pp. 82–91, Jan. 1996.

[37] W. R. Gilks, S. Richardson, and D. J. Spiegelhalter, *Markov Chain Monte Carlo in Practice*, vol. 39, no. 3. 1996.

[38] D. J. Lunn, A. Thomas, N. Best, and D. Spiegelhalter, "WinBUGS – A Bayesian modelling framework: Concepts, structure, and extensibility," *Stat. Comput.*, vol. 10, pp. 325–337, 2000.

[39] A. Haidar, L. Legault, M. Dallaire, A. Alkhateeb, A. Coriati, V. Messier, P. Cheng, M. Millette, B. Boulet, C.-C. Huang, and R. Rabasa-Lhoret, "Glucose-responsive insulin and glucagon delivery (dual-hormone artificial pancreas) in adults with type 1 diabetes: a randomized crossover controlled trial," *Can. Med. Assoc. J.*, p. cmaj.121265–, 2013.

[40] D. J. Lunn, "WinBUGS Differential Interface—worked examples.," *Dep. Epidemiol. Public Heal. Imp. Coll. Sch. Med. London*, 2004.

[41] D. J. Spiegelhalter, N. G. Best, B. P. Carlin, and A. Van Der Linde, "Bayesian measures of model complexity and fit," *J. R. Stat. Soc. Ser. B Stat. Methodol.*, vol. 64, no. 4, pp. 583–616, 2002.

[42] A. D. Cherrington, *Control of Glucose Production in vivo by Insulin and Glucagon*. Hoboken, NJ, USA: John Wiley & Sons, Inc., 2001.

[43] B. A. Finlayson and L. E. Scriven, "The Method of Weighted Residuals - A Review," *Appl. Mech. Rev.*, vol. 19, no. 9, p. 735, 1966.

[44] J. El Youssef, J. R. Castle, P. a Bakhtiani, A. Haidar, D. L. Branigan, M. Breen, and W. K. Ward, "Quantification of the Glycemic Response to Microdoses of Subcutaneous Glucagon at Varying Insulin Levels.," *Diabetes Care*, no. July, pp. 1–7, 2014.

[45] A. Haidar, E. Potocka, B. Boulet, A. M. Umpleby, and R. Hovorka, "Estimating postprandial glucose fluxes using hierarchical Bayes modelling," *Comput. Methods Programs Biomed.*, vol. 108, no. 1, pp. 102–112, 2012.

[46] A. Haidar, D. Elleri, J. M. Allen, J. Harris, K. Kumareswaran, M. Nodale, C. L. Acerini, M. E. Wilinska, N. Jackson, A. M. Umpleby, M. L. Evans, D. B. Dunger, and R. Hovorka, "Validity of triple- and dual-tracer techniques to estimate glucose appearance," *AJP: Endocrinology and Metabolism*, vol. 302, no. 12. pp. E1493–E1501, 2012.

[47] K. Ekberg, B. R. Landau, A. Wajngot, V. Chandramouli, S. Efendic, H. Brunengraber, and J. Wahren, "Contributions by kidney and liver to glucose production in the postabsorptive state and after 60 h of fasting.," *Diabetes*, vol. 48, no. 2, pp. 292–8, Feb. 1999.

[48] D. S. Edgerton, S. Cardin, D. W. Neal, and A. D. Cherrington, "The effect of physiologic changes in insulin on gluconeogenesis in the conscious dog," *Diabetes*, vol. 48, p. (suppl.1) A276, 1999.

[49] A. D. Cherrington, J. E. Liljenquist, G. I. Shulman, P. E. Williams, and W. W. Lacy, "Importance of hypoglycemia-induced glucose production

during isolated glucagon deficiency.," *Am. J. Physiol.*, vol. 236, no. 3, pp. E263–71, Mar. 1979.

[50] R. Parrilla, M. N. Goodman, and C. J. Toews, "Effect of Glucagon: Insulin Ratios on Hepatic Metabolism," *Diabetes*, vol. 23, no. 9, pp. 725–731, Sep. 1974.

[51] M. Wada, C. C. Connolly, C. Tarumi, D. W. Neal, and A. D. Cherrington, "Hepatic denervation does not significantly change the response of the liver to glucagon in conscious dogs.," *Am. J. Physiol.*, vol. 268, no. 2 Pt 1, pp. E194–E203, 1995.

[52] J. Fradkin, H. Shamoon, P. Felig, and R. S. Sherwin, "Evidence for an important role of changes in rather than absolute concentrations of glucagon in the regulation of glucose production in humans.," *J. Clin. Endocrinol. Metab.*, vol. 50, no. 4, pp. 698–703, Apr. 1980.

[53] J. D. Bomboy, S. B. Lewis, W. W. Lacy, B. C. Sinclair-Smith, and J. E. Liljenquist, "Transient stimulatory effect of sustained hyperglucagonemia on splanchnic glucose production in normal and diabetic man.," *Diabetes*, vol. 26, no. 3, pp. 177–4, Mar. 1977.

[54] A. D. Cherrington, P. E. Williams, and M. S. Harris, "Relationship between the plasma glucose level and glucose uptake in the conscious dog.," *Metabolism.*, vol. 27, no. 7, pp. 787–91, Jul. 1978.

[55] V. Batora, M. Tarnık, J. Murgas, and J. B. Jørgensen, "The Contribution

of Glucagon in an Artificial Pancreas for People with Type 1 Diabetes," in *American Control Conference*, 2015.

[56] E. Samols, G. C. Weird, and S. Bonner-Weir, *Intraislet Insulin-Glucagon-Somatostatin Relationships*, vol. 66 / 2. Berlin, Heidelberg: Springer Berlin Heidelberg, 1983.

[57] R. van de Schoot, J. J. Broere, K. H. Perryck, M. Zondervan-Zwijnenburg, and N. E. van Loey, "Analyzing small data sets using Bayesian estimation: the case of posttraumatic stress symptoms following mechanical ventilation in burn survivors.," *Eur. J. Psychotraumatol.*, vol. 6, p. 25216, 2015.

[58] R. L. Dobbins, S. N. Davis, D. W. Neal, C. Cobelli, J. Jaspan, and A. D. Cherrington, "Compartmental modeling of glucagon kinetics in the conscious dog.," *Metabolism.*, vol. 44, no. 4, pp. 452–459, 1995.

[59] J. R. Castle, J. M. Engle, J. El Youssef, R. G. Massoud, K. C. J. Yuen, R. Kagan, and W. K. Ward, "Novel use of glucagon in a closed-loop system for prevention of hypoglycemia in type 1 diabetes.," *Diabetes Care*, vol. 33, no. 6, pp. 1282–7, 2010.